

RESEARCH ARTICLE

Fast successive self-nucleation and annealing (SSA) thermal fractionation protocol for the characterization of polyolefin blends from mechanical recycling

Magdalena Góra^{1,2}  | Davide Tranchida² | Andreas Albrecht² |
Alejandro J. Müller^{3,4}  | Dario Cavallo¹ 

¹Dipartimento di Chimica e Chimica Industriale, Università degli studi di Genova, Genoa, Italy

²Borealis Polyolefine GmbH, Innovation Headquarters, Linz, Austria

³POLYMAT and Department of Polymers and Advanced Materials: Physics, Chemistry and Technology, Faculty of Chemistry, University of the Basque Country UPV/EHU, Donostia-San Sebastian, Spain

⁴IKERBASQUE, Basque Foundation for Science, Bilbao, Spain

Correspondence

Davide Tranchida, Borealis Polyolefine GmbH, Innovation Headquarters, St. Peterstrasse 25, 4021 Linz, Austria.
Email: davide.tranchida@borealisgroup.com

Alejandro J. Müller, POLYMAT and Department of Polymers and Advanced Materials: Physics, Chemistry and Technology, Faculty of Chemistry, University of the Basque Country UPV/EHU, Paseo Manuel de Lardizabal, 3, 20018, Donostia-San Sebastian, Spain.
Email: alejandrojesus.muller@ehu.es

Dario Cavallo, Dipartimento di Chimica e Chimica Industriale, Università degli studi di Genova, via Dodecaneso 31, 16146 Genoa, Italy.
Email: dario.cavallo@unige.it

Abstract

The sorting stage of mechanical recycling of post-consumer polyolefins has severe challenges. Polypropylene (PP) is often contaminated with polyethylene (PE) and vice versa. To meet quality requirements, characterization of the recycled pellets is needed. To address this problem, fast characterization generating a statistical assessment of the content of the various batches from recycling is required. This investigation shows that the use of fast scanning rates (in a conventional Differential Scanning Calorimeter) in the successive self-nucleation and annealing (SSA) protocol can reduce the thermal fractionation time, without losing resolution power, as long as the increase in heating/cooling rate is compensated by reducing sample mass. Using a “coupled SSA protocol” for polypropylene and polyethylene fractions at a rate of 10 °C/min, the measurement time is approximately 420 min. Implementing mass compensation, faster heating rates (i.e., 30 °C/min) and using a single-fraction protocol, sufficient to determine the content of PP and high-density PE, reduced the time of the measurement to 75 min. Examples of fractionations of commercial post-consumer and post-industrial recycled polyolefin blends conducted at a faster rate are provided. The derived polyolefin content is compared with the standard temperature rising elution fractionation analysis to assess the validity of the proposed method.

KEYWORDS

polyethylene, polypropylene, recycling, thermal fractionation

1 | INTRODUCTION

Plastic materials are part of our daily life and our economy. The European Commission's strategy aims to transform the way plastic products are designed, produced, used, and recycled in the EU. The main recycling strategies are primary mechanical recycling, secondary mechanical recycling, tertiary or feedstock recycling, and quaternary recycling.^{1–3} Not all materials can follow the same method of repurposing or recycling. Therefore, separating into different types is one of the key steps to recycling material for new products or components. Mixed materials cannot be reused and reprocessed easily, due to their structural differences.

In the mixed polyolefins (MPO) stream, we have mainly recycled polypropylene and polyethylene, which are incompatible in the melt phase, which leads to phase separation and inferior mechanical properties compared to neat materials.

Mixed polyolefins obtained by mechanical recycling consist of various grades, mainly LDPE, HDPE, PP.^{7,8} Knowing the precise chemical composition of individual batches is essential for processing and compounding. Differential scanning calorimetry (DSC) provides crucial material information, in particular melting and crystallization temperatures, which are valuable for processing. The chemical composition of semi-crystalline post-consumer recycled polyolefin blends can also be evaluated from DSC, based on the melting enthalpy of the different phases.^{9,10}

The existence of branching in the polymer chain, the size of the chain, interactions between the chains, the presence of crystallization promoters (nucleating agents), and other factors all influence crystallization.^{11–13} Industrially applied standard methods to analyze the chemical composition distribution of polyolefins are Temperature Rising Elution Fractionation (TREF),^{14–16} Crystallization Analysis Fractionation (CRYSTAF),¹⁵ and Crystallization Elution Fractionation (CEF). These techniques are based on changes in polymer concentration in solution during temperature reduction via precipitation (CRYSTAF) or after redissolution of the precipitated polymer during increasing the temperature (TREF, CEF).^{18,19} In these standard methods the dissolution step of the sample is typically time-consuming, uses hazardous solvents, and it is often necessary to pre-treat the sample (e.g., filtration of the recycled blend).²⁰ Alternatives based on DSC of bulk samples, on the other hand, have several positive features that speak for them. Examples of these methods are step crystallization (SC) and successive self-nucleation and annealing (SSA). These methods do not use solvents and are therefore cheaper, safer, and typically quicker. The difference between SC and SSA is that, in

the case of SSA, after each high-temperature treatment with an isothermal holding time of 5 min, non-isothermal crystallization ramps to room temperature are performed, which undercools the material and accelerates crystallization, speeding up the entire molecular fractionation process compared to SC.²⁰ Both methods can be used to characterize the crystallizable sequence length in the polymer chain (homopolymer or copolymer) and polymer blends, but there is better segregation and enhanced resolution with the SSA protocol.²¹

Thermal fractionation using the SSA procedure differentiates the material into fractions that are formed as a result of polymer chains defect (branches, tacticity). This sensitivity to the low content of chain defects allows the study of polymer blend miscibility and co-crystallization, cross-linking, ageing, biodegradation, copolymerization, comonomer structure, and SCB distribution.²³

The molecular segregation in SSA is accomplished by several non-isothermal and isothermal stages. The sample is heated to a temperature (T_s) that assures partial melting after an initial heating and cooling phase.²⁰ With lowering T_s , these partial melting processes are repeated and in particular followed by an isothermal phase during which the unmelted lamella anneals and some of the molten chains can isothermally crystallize according to their crystallizable chain length. The last heating run will disclose the thermal fractionation of the materials as a result of the previously applied thermal protocol.²⁰ As established for PE-copolymers, the approach results in remarkably effective molecular segregation.^{23,24} Later, it was also applied to other materials like polypropylene.^{25,26} As for application to the determination of complex compositions of recycled blends, it was first done by Carmeli et al.²⁷ In that study, the authors were able to quantitatively determine the amount of HDPE in the PE-phase and the entire amount of the PP phase.

Few publications have suggested the application of fast heating/cooling rates, which can result in a shorter measurement time. This principle was suggested by the work of Pijpers et al.²⁸ Varga et al. thermally fractionated by step crystallization of low-density polyethylene and high-density polyethylene at a constant rate, but the last heating run was conducted at a different heating rate (20 and 40 °C/min), without finding any significant differences in the obtained results.^{29,30} The concept of using fast rates during the SSA protocol was used by Lorenzo et al., who investigated the application of fast scanning rates on hydrogenated polybutadiene.³¹ Currently, there are no studies about the use of fast heating and cooling rates in complex systems like recycled polyolefin blends. The fast crystallization behaviour of polyolefins allows carrying out measurements on their blends at high heating/cooling rates. Applying fast scanning rates needs

a mass reduction of the sample, to preserve the peak resolution and avoid superheating effects as much as possible. High scanning rates in the SSA protocol can substantially reduce the thermal fractionation time.

In this work, we investigate the applicability of faster SSA thermal protocols to the analysis of the chemical composition of recycled polyolefin blends. After exploring the self-nucleation behaviour of selected blends at different rates to determine the optimal analysis conditions, we introduce a shortened SSA protocol which, while comprising a single fractionation step for the PE and PP phase, still allows the separation of the LDPE and non-crystallizable components from HDPE. Both the standard and the new SSA protocols are applied at different scanning rates, demonstrating no substantial difference in the obtained phase composition among the measurement methods. Finally, the recycled blends are analyzed with the fastest SSA protocol and the outcomes, in terms of compositions, are compared with those of TREF, revealing excellent agreement in practically all cases.

2 | EXPERIMENTAL

2.1 | Materials

Eight materials were obtained from Borealis Polyolefine GmbH (see Table 1). Five materials are coming from post-consumer recycling sources, and are obtained from mechanical recycling. Materials marked with “*m*” are polyolefin mixed recyclates, while those containing “*pp*” in the name are polypropylene dominated recyclates. The approximate composition in percentage is also indicated in the sample code name, for example, m-PE65PP35 indicates a

TABLE 1 List of the used materials in the investigation

Post-consumer recycled blends	Melt flow rate (230 °C/2.16 kg)
<i>m</i> -PE65PP35	5.5 g/10 min
<i>m</i> -PE60PP40	5.5 g/10 min
<i>m</i> -PE40PP60	5.5 g/10 min
<i>pp</i> -PE30PP70	12.5 g/10 min
<i>pp</i> -PE20PP80	20.0 g/10 min
Neat polymers (virgin materials)	Melt flow rate (230 °C/2.16 kg)
HDPE	0.3 g/10 min*
Heterophasic copolymer PP	3.0 g/10 min
Homopolymer PP	6.5 g/10 min

*Melt flow rate (190 °C/2.16 kg).

mixed polyolefin recyclate with approximately 65% of high-density polyethylene and 35% of polypropylene.

The other three materials are neat virgin grades of high-density polyethylene, heterophasic copolymer of polypropylene, and polypropylene homopolymer, which were used as reference materials. Table 1 lists the essential physical parameters of the employed polymers. The thermal properties of the adopted materials are reported, in Table 2.

2.2 | Method of preparation

For some of the blends, a small amount of pellets (about 40 g) was re-blended in a batch mixer (Brabender plastograph), to achieve a good homogeneity of the blend. Mixing was performed at 200 °C for 10 min at 60 rpm.

2.3 | Methods of investigation

2.3.1 | Methodology

Equipment

The SSA protocol, as well as standard melting and crystallization runs, were applied using a TA Instruments Differential Scanning Calorimeter 250. Measurements were carried out at heating and cooling rates of 10, 20, and 30 °C/min. The temperature limits of the linear ramps were 20 and 200 °C.

In order to compare the blend composition results obtained by the SSA protocols with a different quantification method, TREF was used as an industrial standard. Measurements were performed using the Polymer Char device Crysaf-TREF 200+.

Sample preparation

Samples for the DSC measurement were firstly compression moulded to obtain a thin film from the pellets. From that thin film, a small disk was made, with a 4-millimetres hole punch, to get a flat sample for the analysis. This sample size matches perfectly with the pan, which was used in the investigation, a T_{zero} pan, for having good contact with the sensor inside the device. To get the proper weight, needed for the mass compensation experiment, the sample was then cut to the required size (corresponding to weights of approximately 1, 2, and 3 mg).

Samples for TREF were used as received after sample preparation (2.2). In particular, to avoid injecting possible gels and/or polymers which do not dissolve in TCB at 160 °C, like PET and PA, the weighed sample was packed into a stainless steel mesh MW 0.077/D 0.05 mm. About

TABLE 2 List of the used materials in the investigation with temperatures of crystallization and melting of the different phases. Measurements of non-fractionated materials were performed at 30 °C/min

Material	T_c	ΔH_c	T_m	ΔH_m	T_c	ΔH_c	T_m	ΔH_m
	PE [°C]	PE [J/g]	PE [°C]	PE [J/g]	PP [°C]	PP [J/g]	PP [°C]	PP [J/g]
Homopolymer PP	-	-	-	-	124.2	113.5	165.0	113.3
Heterophasic copolymer PP	-	-	-	-	124.7	104.1	165.6	106.8
HDPE	113.1	177.8	127.6	182.2	-	-	-	-
<i>m</i> -PE65PP35	112.8	67.8	125.3	70.7	118.9	32.3	158.9	36.1
<i>m</i> -PE60PP40	114.0	73.8	126.4	72.9	119.4	34.5	159.2	38.8
<i>m</i> -PE40PP60	102.0	50.3	126.2	47.0	118.4	48.2	158.9	54.1
<i>pp</i> -PE30PP70	-	-	125.1	16.8	118.1	87.1	160.2	71.9
<i>pp</i> -PE20PP80	-	-	125.5	26.7	120.2	96.4	160.5	76.8

50 mg of the polymer sample have been dissolved in 40 ml 1,2,4-trichlorobenzene (TCB), stabilized with 250 mg/L 2,6-di-tert-butyl-4-methyl-phenol (BHT), for 2 h at 160 °C.

2.3.2 | Measurement procedures

Standard runs

Standard DSC measurements were carried out at a heating and cooling rate of 10 °C/min from 20 to 200 °C. Determination of melting and crystallization temperatures and enthalpies were measured from the second heating and cooling curves.

T_s ideal selection

The previous thermal history was removed by heating the sample to 200 °C. Then, the material was cooled down to 20 °C at a chosen rate, to create a standard crystalline state. After cooling, the material was heated to a temperature T_s where the isothermal treatment was applied for 5 min. This isothermal treatment can cause: (a) complete melting, if T_s is much higher than the melting point (T_m) (*Domain I* or complete melting *Domain*); (b) melting of most of the crystals but leaving small crystal fragments or ordered regions in the melt that act as self-nuclei (*Domain II* or self-nucleation *Domain*); (c) partial melting that will cause annealing of unmolten crystals during the 5 min of thermal treatment at T_s (*Domain III* or self-nucleation and annealing *Domain*). The material was then cooled to 20 °C at a constant rate. After that step, the material was finally heated to 200 °C again. A final heating run will display any changes in the melting behaviour of the material caused by the self-nucleation treatment. If the sample is in *Domain II* only minor changes are usually observed in the melting endotherm with respect to a sample in *Domain I*. However, if

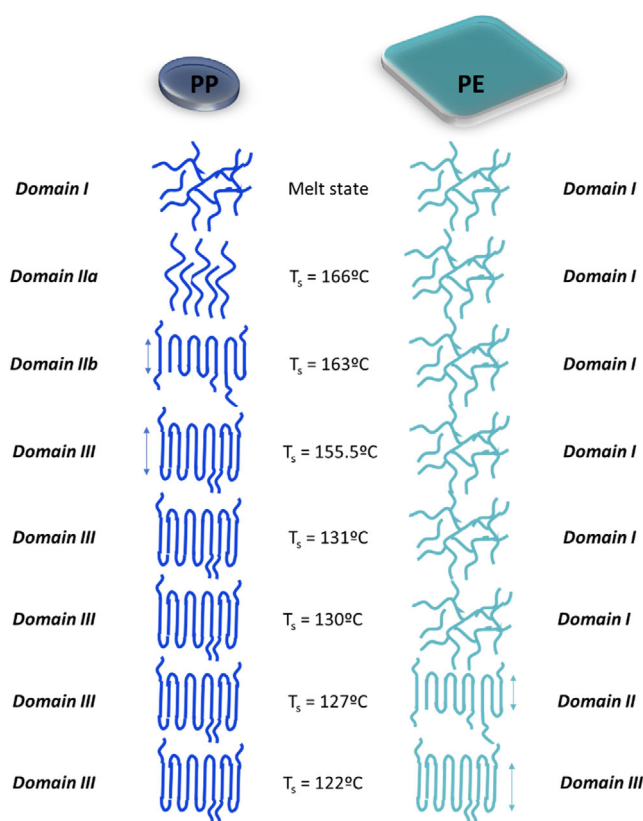


FIGURE 1 Graphical representation of the PP/PE blend under certain temperatures and related domains of the two components. The presented temperatures are examples of typical values of a real blend.

the sample is in *Domain III*, an additional high temperature melting peak will appear, due to the melting of the annealed crystals at T_s . Hence, this heating step is necessary to detect if the sample is in *Domain III* or not. Also, changes during the cooling run from the T_s , will be observed. When the polymer changes its crystallization temperature (T_c) to a higher value, the material underwent self-nucleation during isothermal treatment at T_s .

More nucleation centres increase the T_c , which is the desired effect. $T_{s,ideal}$ is then found by knowing the boundary between *Domain III* (self-nucleation and annealing) and *Domain II* (exclusive self-nucleation). The ideal self-nucleation temperature ($T_{s,ideal}$) is the lowest temperature within *Domain II* and it is defined as the temperature that produces the highest number of self-nuclei in the sample without causing any annealing.

Domain II is subdivided into two subdomains. *Domain IIa* occurs when the T_s temperature is high enough to melt all crystals in the sample (i.e., no latent heat of melting can be detected in *Domain IIa* but low enough to leave certain ordered regions in the melt that can act as self-nuclei upon the following cooling. *Domain IIb* is defined by a T_s temperature that is high enough to nearly melt the entire sample but low enough to leave small crystal fragments unmolten, that can represent self-seeds (but are not annealed), as shown in Figure 1.^{33,34}

For the recycled polyolefins blends containing polypropylene and polyethylene, the self-nucleation can be conducted as described above, without changes in the protocol, because the temperature treatment applied to PP, while slightly affecting the crystallization temperature of PE, does not meaningfully change the fractionation outcome of the low melting polymer.²⁸ The opposite, that is, no effect of PE thermal treatment on PP fractionation, is also true, as demonstrated by Carmeli et al. (see fig. 5, Reference 28). The applied temperature during the self-nucleation protocol, for the polypropylene ($T_{s,ideal}$ 163.0 °C) corresponds to having polyethylene always in *Domain I*. On the contrary, when self-nucleation is applied to polyethylene ($T_{s,ideal}$ = 127.0 °C) the polypropylene phase will be in *Domain III*. This concept is graphically represented in Figure 1, which reports representative temperature ranges for Self-nucleation of the two phases with the respective self-nucleation domains.

The steps of defining $T_{s,ideal}$ needs to be conducted and repeated for every blend and cooling/heating condition used in this study. In fact, different ratios of the phases in the blend, as well as the used heating/cooling rates might change the values of the melting and crystallization temperature, and therefore $T_{s,ideal}$ as well. The $T_{s,ideal}$ for polypropylene and polyethylene defined in this stage, for the different compositions and cooling/heating rates, are then later used in the SSA protocol, see below.

SSA multi-fraction protocol (“coupled SSA protocol”)

The sample was heated 30 °C above the melting temperature to remove thermal history and then cooled down to room temperature under controlled cooling at the chosen rate. From this temperature, the sample was heated to the $T_{s,ideal}$ (description of the T_s , ideal selection above),

and kept at this temperature for 5 min. As the next step, the temperature was lowered to room temperature to obtain the standard crystalline state. Following this step, the material was heated to $T_{s,1}^{PP}$, which was 7.5 °C lower than the $T_{s,ideal}$ for the polypropylene fraction. The 7.5 °C fractionation window was chosen based on a previous optimization.²⁸ Then again, the sample was cooled down to room temperature. The fractionation window was lowered 4 times from the $T_{s,ideal}$, which allowed the production of four fractions from the PP phase. As for the polyethylene phase, the material is heated to the $T_{s,ideal}$ of the polyethylene chosen before, and kept at this temperature for 5 min. From this temperature, it is cooled down to room temperature. The next step requires heating the sample to a temperature of 5 °C lower than T_s ideal for the polyethylene fraction ($T_{s,1}^{PE}$), based on previous studies.²¹ Later, the sample is cooled down to room temperature. The steps including lowering the temperature by 5 °C and then cooling from that temperature to 20 °C were repeated eight times, which allowed the production of eight fractions for the polyethylene phase. The last heating step, with the same rate as all the previous steps, goes to 200 °C. In this measurement step, the melting points from the fractions produced during the applied protocol are observed. In this fractionation protocol, the material was fractionated into 12 thermal fractions.

SSA single-fraction protocol

The single fraction methodology follows the same measuring principles as the multi-fraction protocol previously mentioned. The difference is in the number of temperature steps. The single-fraction protocol creates only one fraction from each of the two materials under consideration, namely high-density polyethylene and polypropylene. This single fraction is obtained after thermal treatment at $T_{s,ideal}$ and $T_{s,1}$ for both materials. Furthermore, the fractionation window remains the same with respect to the multi-fraction protocol.

The protocol only uses a single fractionation step (i.e., isothermal treatment at $T_{s,1}$) for each component of the blend (apart from the self-nucleation step at $T_{s,ideal}$, which does not produce fractionation, only self-nucleation of the sample), as it has been demonstrated that the highest temperature fraction of the PE phase is unaffected by co-crystallization phenomena with LDPE.²⁸ Figure 2 shows the comparison between the abbreviated single fraction SSA thermal procedure and full treatment.

TREF measurement protocol

The a-TREF analysis was carried out using Crystef-TREF 200+ PolymerChar instrument, equipped with an infrared concentration detector. An aliquot of the prepared solution was injected onto the TREF column

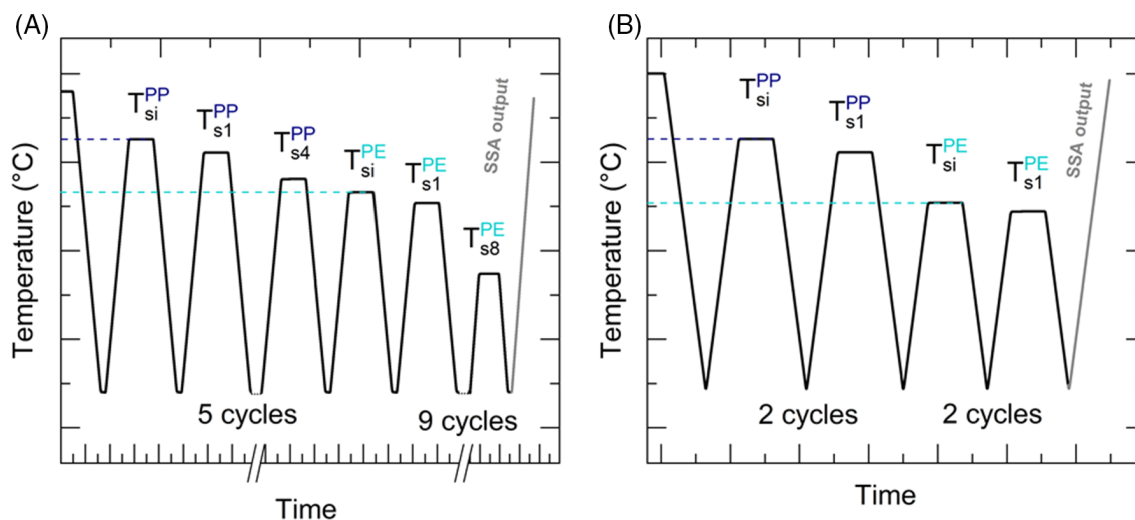


FIGURE 2 (A) Fractionation program implemented and designed by Carmeli et al., which uses 14 cycles to obtain eight fractions for the polyethylene part and four fractions for the polypropylene phase³⁹ (B) fractionation program designed for the calculation of the main types of the polyolefins: HDPE and PP, which uses four cycles of temperature treatments and results in two fractions, one for the polypropylene part and the second one for high-density polyethylene.

and stabilized for 30 min at 110 °C. After the stabilization, the temperature was lowered to 35 °C after stabilization using a constant cooling rate of 0.1 °C/min. A flow rate of 0.5 ml/min at 35 °C for 10 min was used to collect the soluble fraction, followed by a temperature ramp from 35 to 140 °C at a continuous heating rate of 0.5 °C/min and a flow rate of 0.5 ml/min. The concentration of the eluted fraction and the corresponded signal is determined with the detector and plotted as a function of temperature.

2.3.3 | Data analysis

Data from the standard run

For the polypropylene, the crystallization and melting enthalpy were calculated from the baseline, which was chosen from the onset of the polyethylene phase melting till 180 °C. On the other hand, for the polyethylene, the crystallization and melting temperature and enthalpy were calculated from the baseline starting from 40 °C till the beginning of the polypropylene phase. In the neat materials, the baseline was fixed from 40 to 180 °C, except for neat polypropylene where the baseline ended at 200 °C.

Area calculation

The heat flow rate values were divided by the heating/cooling rate to calculate the apparent heat capacity values. These normalized data points were imported into the OriginLab software. In the Origin Lab software, the

data from the single fraction protocol was analyzed in the following way:

1. data was imported to the peak analyzer application,
2. baseline values were set to be 40–180 °C,
3. the two highest peaks were selected manually,
4. boundaries for the area integration for polyethylene were set to be at the minima before and after the peak for polyethylene, and for polypropylene, constant temperature boundaries of 136–180 °C were set.

The same methodology has been implemented for the characterization of all materials. The content of a given polymer in the recycled fraction was calculated using a proportion with respect to the area under the melting peak, with the maximum area constituted by the reference materials, that is, virgin polymer. For polypropylene, the reference value was calculated as the average of heterophasic and homopolymer polypropylene melting peak area, given the different possible types of polypropylenes in real recycled grades. For the high-density polyethylene phase, a grade for film extrusion was used as reference material.

α-TREF analysis

From TREF analyses the normalized concentration plot (dW/dT) together with the cumulative concentration signal normalized to 100 along the temperature were retrieved. The different polymer types were assigned according to their elution temperature in α-TREF. The polymer fraction eluting between 35 and 90 °C, which mainly comprises low-density polyethylene and PE fraction with a higher

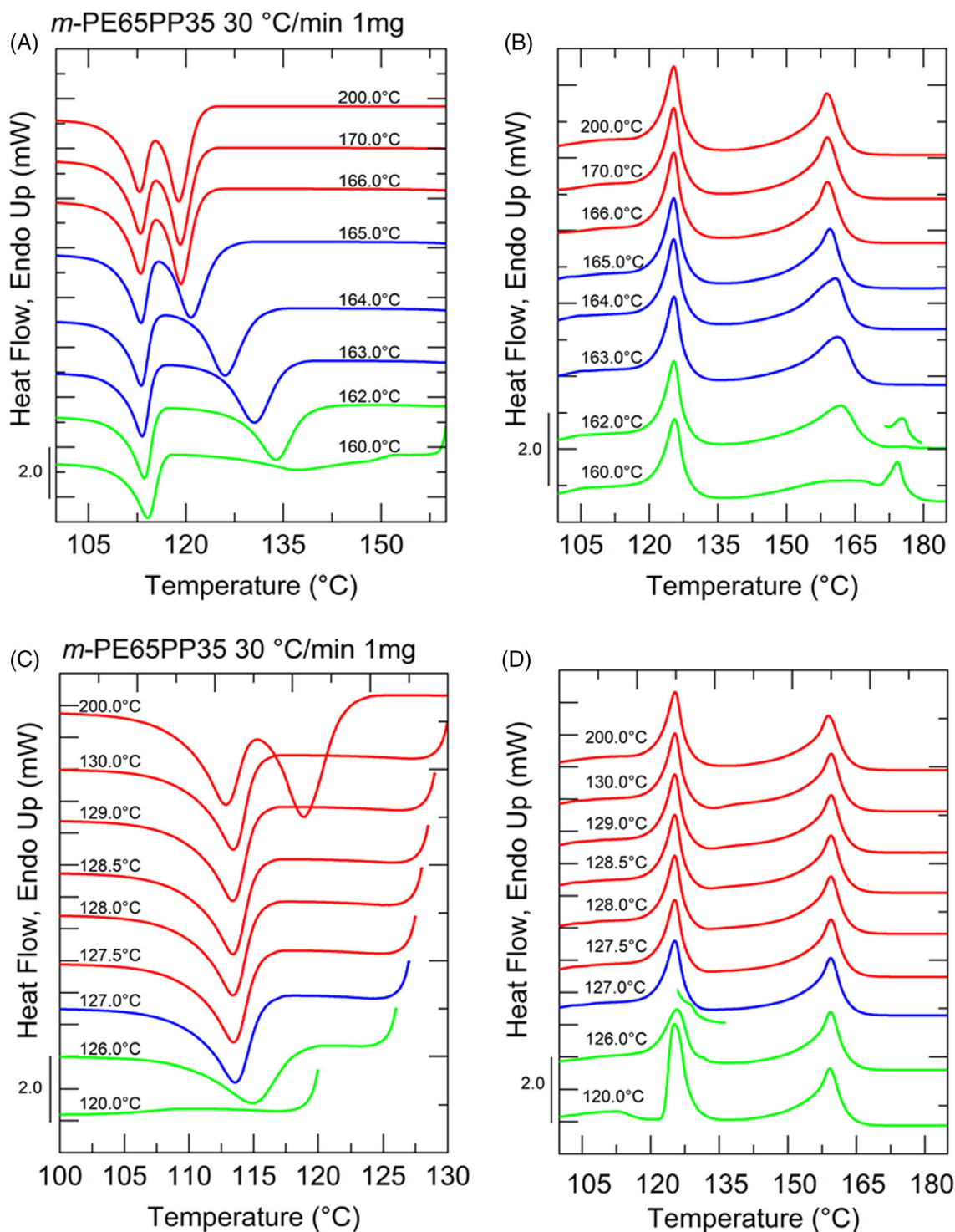


FIGURE 3 $T_{s,ideal}$ selection for m-PE65PP35 (A) DSC cooling scans at 30 °C/min after 5 min at the indicated T_s for polypropylene in recycled polyolefin blend (B) subsequent heating scans (at 10 °C/min) after cooling runs shown in (A). (C) DSC cooling scans at 30 °C/min after 5 min at the indicated T_s for polyethylene in recycled polyolefin blend (D) subsequent heating scans (at 30 °C/min) after cooling runs shown in (C) colours of the lines in the graphs indicating material under certain domains: Red lines—*Domain I*, blue lines—*Domain II*, green lines—*Domain III*. The occurrence of an annealing peak in the PE and PP phase is highlighted as a separate inset next to the corresponding curve. The curves are colour-coded to indicate the different SN domains: Red for *Domain I*, blue for *Domain II*, and green for *Domain III*.

content of short-chain branches but also low molar mass PE and PP, is defined as LDPE/LLDPE fraction. The fraction eluting between 90 °C and 103 °C, which mainly

contains homo-PE chains and PE chains with low branching content, is named high-density polyethylene fraction where the fraction eluting above 103 °C is defined as

polypropylene fraction and the fraction below 35 °C as soluble fraction. For materials with higher polypropylene content (*pp*-PE30PP70 and *pp*-PE20PP80), the temperature range was changed for the polypropylene fraction from 100 to 130 °C and the high-density polyethylene fraction between 90 and 100 °C because the elution of the polypropylene starts at lower temperatures. All the other fractions and their temperature ranges remain unchanged.

3 | RESULTS AND DISCUSSION

3.1 | Standard runs

When taken from different pellets, the DSC measurement showed differences in the enthalpy of fusion for the samples *m*-PE65PP35, *m*-PE40PP60, and *pp*-PE30PP70. Therefore, those blends were homogenized. After melting and blending in a batch internal mixer, three tests on the DSC were performed for each homogenized blend. Figure S1 presents the DSC results of blends before and after homogenization. The differences observed among the curves in Figure S1a–c plots are largely reduced after homogenization (Figure S1d–f). The other two materials were homogeneous as supplied and did not need re-mixing.

3.2 | Self-nucleation and $T_{s,ideal}$ selection

As an example, the DSC heating and cooling curves for *m*-PE65PP35, following isothermal treatments at T_s for 5 min are shown in Figure 3.

In Figure 3A, cooling from 200 °C, resulted in a crystallization temperature of the polypropylene phase at 119.0 °C. Other experiments found that isothermal treatment at T_s between 165 and 163 °C led to a significant increase in the crystallization temperatures, from 119.2 to 130.7 °C. Treatment at different T_s values did not change the melting peak significantly (Figure 3B), but slight changes in the shape of the peak were observed for T_s in *Domain II*. However, when T_s is equal to 162 °C, the subsequent heating run revealed an additional melting peak around 175.7 °C. As such, $T_{s,ideal}$ can be defined as the lowest T_s value within *Domain II*, which for this specific case is 163 °C.

Figure 3C) shows that the polypropylene crystallization peak does not appear when the material is crystallized from 130.0 °C downwards, while it is still present if the cooling run starts from 200 °C. No change in the crystallization temperature of the PE phase (113.4) was observed when experiments were done at T_s values between 130.0 and 127.5 °C. However, T_c increased

slightly after treatment at $T_s = 127.0$ °C from $T_c = 113.4$ to $T_c = 113.6$ °C. Because the difference of 0.2 °C is modest and within the measurement error range, *Domain II* in this mixed polyolefin system for the polyethylene phase is assumed to be absent.

In high-density polyethylene copolymers, Carmeli et al. found a narrow *Domain II* for high-density polyethylene.³⁵ In other studies, high-density polyethylene homopolymer and polyethylene blocks inside copolymers were shown to possess just *Domain I* and *Domain III*.^{36,37} The authors attributed *Domain's II* complete absence to the high-density polyethylene's extraordinarily high number of active heterogeneities, which prevent self-nucleation from causing any further increases in nucleation density. For $T_s = 126.0$ °C there was a significant change in the T_c value which raised to 115.2 °C. Therefore, the $T_{s,ideal}$ was chosen as 127.0 °C. This is the lowest temperature, which does not cause the annealing of the polymer lamellae.

In Figure 3D, post-crystallization heating from 200.0 °C yields a melting temperature of 125.4 °C. The runs after treatment at selected T_s experiments did not show a significant trend in the melting point. However, after treatment at 126.0 °C, an additional peak was obtained around 132.0 °C. Therefore, $T_{s,ideal}$ for the PE phase is identified as 127.0 °C.

Defining $T_{s,ideal}$ might be a difficult task when the majority of the phase is polypropylene, whose tail might be overlapping with the melting temperature range of HDPE. In this case, the annealing peak appears on top of the low-temperature tail of polypropylene (see Figure S2).

3.2.1 | Influence of the scanning rate

Each adopted heating and cooling rate in the thermal protocol resulted in a different $T_{s,ideal}$, see Figure 4. The polypropylene phase T_s ideal shifts from 166.0 °C at

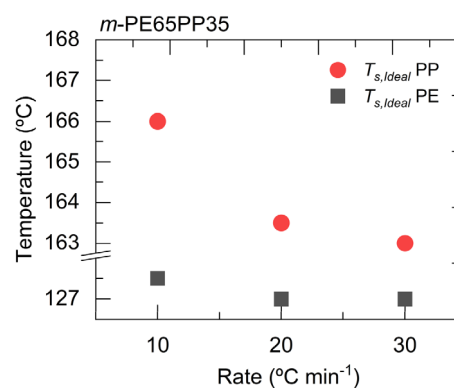


FIGURE 4 $T_{s,ideal}$ values selected for the PE and PP fractions present in the recycled blend for *m*-PE65PP35, as a function of the change in the heating/cooling rate.

10 °C/min, to 163.0 °C at 30 °C/min. For the polyethylene phase, the change is only minor, that is, from 127.5 °C at 10 °C/min to 127.0 °C at 30 °C/min. The obtained results for all the analyzed blends are in Figure S3. The variation of $T_{s,ideal}$ with cooling rate is associated with the corresponding variation of the crystalline standard state, as a consequence of the changes in crystallization temperature at different rates of cooling. Considering that the dependence of polypropylene and polyethylene crystallization kinetics on undercooling and the self-nucleation behaviour of the two polymers are different, the observed different trend of $T_{s,ideal}$ with cooling rate is understandable. In particular, it must be reminded that PP has much less active nucleating heterogeneities than PE, so the crystallization kinetics is more sensitive to cooling rate. Moreover, in PP the crystallization temperature can be increased with self-nucleation much more than in the PE case, because of the lower density of active nuclei. So the small amount of change in crystallization temperature with self-nucleation for PE is reflected in the lower change in $T_{s,ideal}$.

3.3 | Comparison between the two SSA protocols employed

In Figure 5A, the black DSC trace represents data from the multi-fraction protocol (coupled SSA protocol). The result of the measurement shows 8 well-defined melting peaks between 90.0 and 132.0 °C corresponding to the eight thermal fractions produced by SSA in the PE phase. The melting peaks appear every 5 °C as expected (i.e., a fractionation window of 5 °C was employed for the PE phase), and they have different heights and areas, according to the population of the respective crystallizable units in the fraction. Branches interrupt the linear crystallizable sequences in the chains leading to the formation of thinner lamellae that melt at lower temperatures. The higher the branch content, the lower the melting point of the corresponding fraction. Each fraction can be quantified by the area under each peak, or the corresponding melting enthalpy. Concerning polypropylene, there are four peaks between 136.0 and 172.0 °C that represent the four thermal fractions produced by the SSA protocol. The first two peaks at lower temperatures are not well pronounced, but the following ones at 158.5 and 168.5 °C stand out.

In Figure 5A, the red DSC curve represents the result of the single-fraction SSA protocol. The measurement shows a single broad peak in the lower temperature range between 80.0 and 125.0 °C, and a second sharp one at around 125.0–132.0 °C. The sharp peak is produced by the thermal fractionation performed at $T_{s,1}$ for PE. The

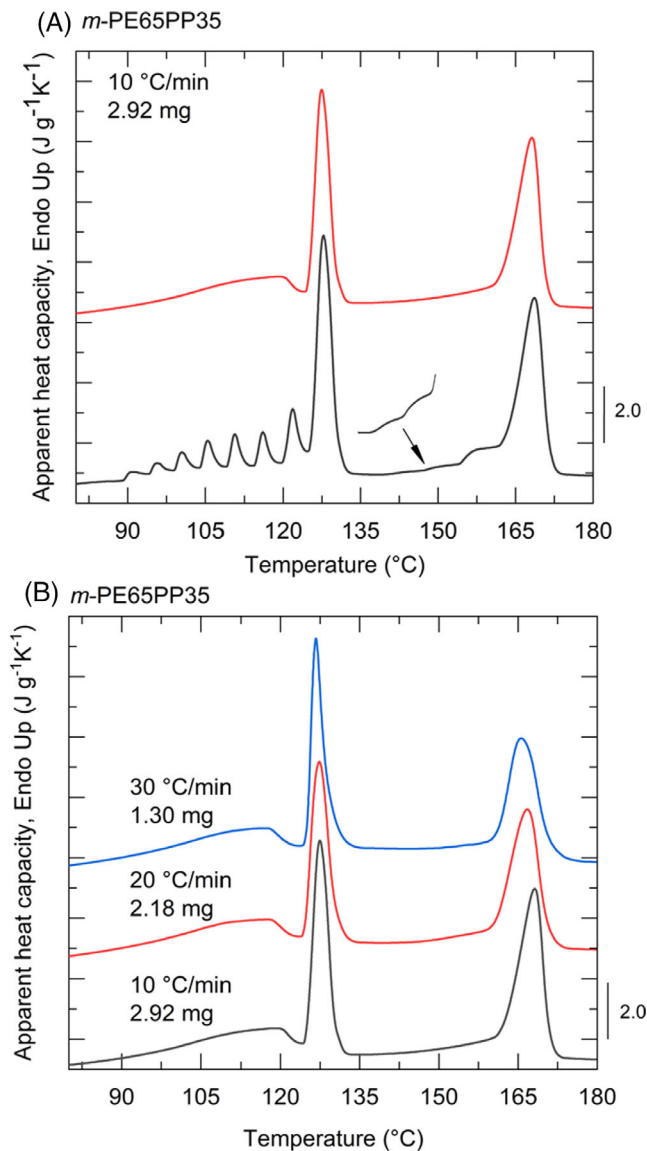


FIGURE 5 (A) Comparison of the outcome of the two SSA fractionation protocols for m-PE65PP35: The DSC curve in red corresponds to the single-fraction and the one in black to the multi-fraction protocol (B) comparison of single-fraction protocols under different heating/cooling rates, the rates and sample masses are indicated in the inner legend.

second, low-temperature broad peak corresponds to the melting of the unfractionated part of the PE phase. These two peaks probably correspond to the LDPE fraction (possibly co-crystallizing with HDPE) and to the neat HDPE, at low and high temperatures, respectively.

In the case of the PP phase, the single SSA fractionation protocol produces a sharp melting fraction in the range 160.0 to 172.0 °C. The unfractionated part of the PP phase melts in the tail of the main fractionated peak located between 136.0 and 160.0 °C.

Figure 5B reports the results obtained after applying the SSA single fraction protocol at different cooling and

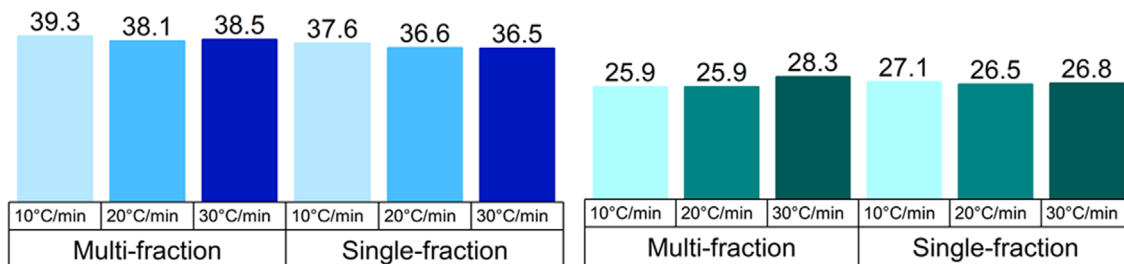
(A) PP Content - *m*-PE65PP35(B) HDPE Content - *m*-PE65PP35

FIGURE 6 *m*-PE65PP35 (A) content of the polypropylene and (B) polyethylene calculated from different measurement rates and protocols (values of the bars are presented in % and the groups under the bars are related to the protocol used for the measurement, example: Multi-fraction protocol at 10 °C/min—39.3% of polypropylene).

heating rates. It can be seen that the overall appearance of the SSA fractionation curves keeps similar, despite the changes in the scanning rate. The melting peaks are slightly shifted to lower temperatures with a faster heating rate, indicating that the crystals might possess less time to reorganize themselves into thicker lamellae during the heating phase. This effect could also possibly be due to a lower crystallization temperature of the polymers in the cooling step. On the other hand, the area calculation results are not affected by the shift of the melting peak since the reference material was subjected to the same temperature program using the same heating/cooling rate. Moreover, the resolution of the peaks seems relatively unaffected using higher heating rates, as well as the relative area, which appears similar between the different runs, at a first qualitative inspection.³⁸

To confirm the qualitative indication regarding the area of the fractionation peaks, proportional to the content of PP and HDPE phases, the results obtained from calculating the areas under the peaks were pooled and compared together, among different SSA protocols and rates (Figure 6). The results from the multi-fraction SSA protocol were compared at different cooling and heating rates with the results from the single-fraction SSA protocol also at different rates.

For the selected blend, considered as an example, the calculated content is substantially independent of both the type of protocol selected and the heating/cooling rate adopted. This result validates the method and anticipates that meaningful timesaving can be gained by performing all the analyses with the single-fraction protocol and a rate of 30 °C/min.

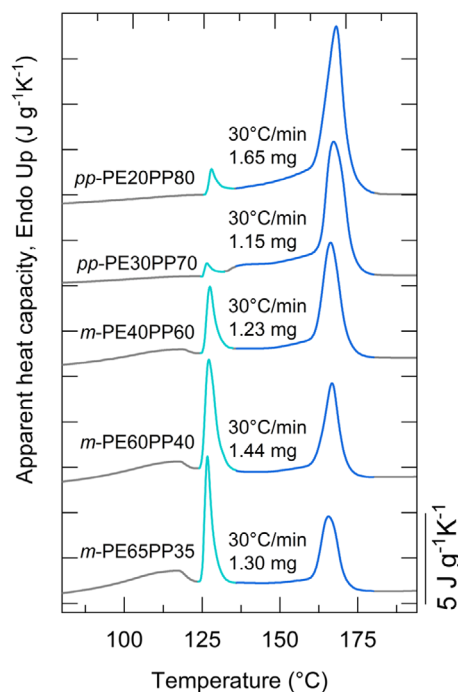


FIGURE 7 Fractionation output run results for the investigated materials. The content of PP decreases from top to bottom, while that of PE correspondingly increases in the same direction.

3.4 | Results from the single-fraction SSA protocol

In Figure 7, the results of the single-fraction SSA protocol applied at 30 °C/min are presented. The data are arranged with decreasing content of PP in the blends

TABLE 3 Results of the composition calculations from the single-fraction protocol (at 30 °C/min heating/cooling rate). All values are displayed as percentages

Material	PP SSA [%]	PP a-TREF [%]	HDPE SSA [%]	HDPE a-TREF [%]	LDPE + others SSA [%]	LDPE a-TREF [%]	Soluble fraction a-TREF [%]
<i>m</i> -PE65PP35	36.5	35.9	26.8	27.1	36.7	29.7	7.3
<i>m</i> -PE60PP40	39.9	37.7	30.0	28.8	30.1	26.1	7.7
<i>m</i> -PE40PP60	58.0	55.1	16.0	19.8	29.0	16.3	8.7
<i>pp</i> -PE30PP70	71.8	80.8	3.4	5.3	24.8	3.8	10.1
<i>pp</i> -PE20PP80	83.5	82.4	5.7	7.6	10.8	0.0	10.0

from top to bottom. The PE fraction correspondingly increases (notice the increase in melting peak areas of the PE phase in the temperature range of 80.0–135.0 °C) in the same direction. It can be seen that only the materials with the highest PE fraction develop a third peak at low temperature upon fractionation, attributed to low-density polyethylene. Material with high PP content possesses a low-temperature melting tail of the polypropylene peak that partially overlaps with the HDPE melting peak. For one material, *pp*-PE30PP70, besides this low melting tail, a distinct third fraction is found in between HDPE and PP, possibly generated upon the annealing at $T_{s,ideal}$ of HDPE. This third fraction can tentatively be ascribed to low-tacticity/high comonomer content PP chains.³⁹

The single-fraction SSA protocol was run three times on one of the blends at 30 °C/min heating/cooling rate to calculate the repeatability of the area integration. The outcome is a precision of 1.3% for the PP phase and 0.6% for the HDPE phase. The data used for this calculation are shown in Figure S4.

3.5 | Comparison with TREF

All the results of the compositional analysis for the PP and HDPE contents obtained by the fastest SSA protocol (i.e., the single-fraction SSA protocol performed at 30 °C/min scanning rates) are summarized in Table 3, where they are compared with analytical TREF derived compositions on the same blends. The content of “LDPE+others” from SSA is simply derived by the complement to 100%, taking into account the percentages of PP and HDPE. In general, a very good agreement between the two techniques is found. To better visualize the discrepancies, the differences between TREF and SSA results are plotted as a histogram in Figure 8.

The differences in the obtained results between SSA and a-TREF are particularly small for *m*-PE65PP35 and are comprised within 4% for all the blends, with one exception. In fact, an error of 10.9% was obtained for *pp*-

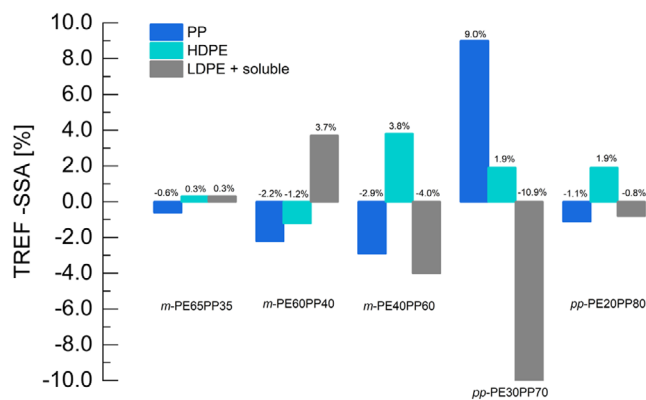


FIGURE 8 Difference between the TREF and SSA compositions. Each triplet of bars corresponds to a particular investigated material as indicated on the x-axis.

PE30PP70, in the content of polypropylene, which in turn caused a high error in the content of “LDPE + soluble” as well.

The reason behind the large discrepancy of *pp*-PE30PP70 might be found in the small peak between HDPE and PP fractionation peaks in the SSA results, see Figure 7. This peak cannot be detected in the standard run, which means that it arises during the lower temperature annealing steps of the SSA protocol. As previously described, the peak can be tentatively attributed to random propylene-ethylene copolymers, either crystallizing alone or co-crystallizing with the low-melting fraction of *i*-PP homopolymer.⁴⁰ Figure S5 presents the result of the a-TREF measurement on the *pp*-PE30PP70 blend. Shorter chains of the low isotacticity polypropylene can elute at 60.0–80.0 °C, and therefore there can be an underestimation from the a-TREF results of the polypropylene content.⁴¹ A slight overestimation of the high-density polyethylene can also be produced by chains from the polypropylene, which might elute at the temperature of 90.0 °C together with the high-density polyethylene fraction. In general, co-elution is a problem of a-TREF, which is influenced by the experimental conditions.^{42,43} For most studied blends (except *m*-PE60PP40), the results

of HDPE from a-TREF are estimating a higher content than from SSA. Where as the polypropylene derived via a-TREF has a lower content than that obtained from the SSA protocol. Both effects of lower PP content and higher HDPE content can be explained partially by the co-elution of low molar mass PP with the HDPE and LDPE fraction in TREF. It is apparent that there is not a unique way of defining the blend composition, but each technique, that is, TREF and SSA, has its drawbacks and strengths. Nevertheless, even considering a general agreement within 10% as a worst-case scenario indicates that the faster single-fraction SSA protocol proposed in this work is a successful alternative to a-TREF, leading to faster results in less time and without the use of solvents.

4 | CONCLUSIONS

Higher rates of heating/cooling during SSA thermal fractionation can be applied to commercial recycled polyolefin blends, provided that a mass compensation principle is adopted. Lowering the mass reduces the possibility of thermal inertia.

It is beyond the scope of the study to calculate the LDPE content in post-consumer blends since HDPE and LDPE can undergo partial co-crystallization in this system. This problem arises as well in the fractionation performed with other crystallization-based techniques, such as TREF, CRYSTAF and CEF.

In conclusion, the faster single-fraction SSA protocol proposed in this work is an easy and inexpensive method to be applied to recycled materials to characterize their crystallization properties and the chemical content of individual polymers in a blend. This study proved that the measurement results do not lose their quality if faster scanning rates (as applied in conventional DSC equipment) are used. Using faster cooling/heating rates enables for more measurements to be taken in the same amount of time. In fact, the SSA protocol can be tailored according to the required outcome. A full fractionation using the rate of 10 °C/min takes about 420 min, while the production of a single fraction for the two phases at the rate of 30 °C/min lasts about 75 min. SSA can be used to determine the composition of recycled materials faster than a-TREF, while the precision is comparable.

ACKNOWLEDGMENTS

The authors acknowledge the financial support from the REPOL project; this project has received funding from the European Union's Horizon 2020 research and innovation program under the Marie Skłodowska-Curie Grant Agreement No. 860221. Furthermore, the authors would

like to thank Enrico Carmeli for training M.G. and Vitor Barroso for supervision in the early stage of this study.

ORCID

Magdalena Góra  <https://orcid.org/0000-0001-7055-7785>

Alejandro J. Müller  <https://orcid.org/0000-0001-7009-7715>

Dario Cavallo  <https://orcid.org/0000-0002-3274-7067>

REFERENCES

- [1] Z. O. G. Schyns, M. P. Shaver, *Macromol. Rapid Commun.* **2021**, *42*, 2000415. <https://doi.org/10.1002/marc.202000415>
- [2] J. Hopewell, R. Dvorak, E. Kosior, *Phil. Trans. R. Soc. B* **2009**, *364*, 2115.
- [3] V. Beghetto, R. Sole, C. Buranello, M. Al-Abkal, M. Facchin, *Materials* **2021**, *14*, 4782.
- [4] J. M. Eagan, J. Xu, R. Di Girolamo, C. M. Thurber, C. W. Macosko, A. M. LaPointe, F. S. Bates, G. W. Coates, *Science* **2017**, *355*, 814.
- [5] A. Van Belle, R. Demets, N. Mys, K. Van Kets, J. Dewulf, K. Van Geem, S. De Meester, K. Ragaert, *Polymer* **2020**, *12*, 1171.
- [6] M. Xanthos, *Science* **2012**, *337*, 700.
- [7] H. Jones, F. Saffar, V. Koutsos, D. Ray, *Energies* **2021**, *14*, 7306. <https://doi.org/10.3390/en14217306>
- [8] F. Alvarado Chacon, M. T. Brouwer, E. U. Thoden van Velzen, I. W. Smeding, *Wageningen Food & Biobased Research* **2020**, *2030*, 34. <https://doi.org/10.18174/518299>
- [9] W. Camacho, S. Karlsson, *Polym. Eng. Sci.* **2001**, *41*, 1626.
- [10] Å. G. Larsen, K. Olafsen, B. Alcock, *Polym. Test.* **2021**, *96*, 107058. <https://doi.org/10.1016/j.polymertesting.2021.107058>
- [11] M. Zhang, B.-H. Guo, J. Xu, *Crystals* **2016**, *7*, 4.
- [12] J. Xu, G. Reiter, R. Alamo, *Crystals* **2021**, *11*, 304. <https://doi.org/10.3390/cryst11030304>
- [13] C. E. Carraher, R. B. Seymour, in *Seymour/Carraher's Polymer Chemistry*, 6th ed. (Ed: M. Dekker), Undergraduate Chemistry, New York **2003**.
- [14] J. B. P. Soares, A. E. Hamielec, *Polymer* **1995**, *36*, 1639.
- [15] S. Anantawaraskul, J. B. P. Soares, P. M. Wood-Adams, Fractionation of Semicrystalline Polymers by Crystallization Analysis Fractionation and Temperature Rising Elution Fractionation. in *Polymer Analysis Polymer Theory*, Vol. 182 (Eds: A. Abe, K. Dušek, S. Kobayashi), Advances in Polymer Science; Springer Berlin Heidelberg, Berlin, Heidelberg **2005**, p. 1.
- [16] L. Wild, G. Glöckner, Proceedings of the Separation Techniques Thermodynamics Liquid Crystal Polymers, Springer Berlin Heidelberg, Berlin, Heidelberg, 1991, 1.
- [17] B. Monrabal, J. Sancho-Tello, N. Mayo, L. Romero, *Macromol. Symp.* **2007**, *257*, 71.
- [18] J. Soares, T. Mckenna, Polyolefin Microstructural Characterization. in *Polyolefin Reaction Engineering*. Vol Verlag Gmb, 1st ed. Wiley-VCH, Weinheim, Germany **2012**, pp.5–52.
- [19] B. Monrabal, Polyolefin Characterization: Recent Advances in Separation Techniques, in *Polyolefins: 50 years after Ziegler and Natta I*, Vol. 257 (Ed: W. Kaminsky), Advances in Polymer Science; Springer Berlin Heidelberg, Berlin, Heidelberg **2013**, pp. 203–251.

- [20] A. J. Müller, M. L. Arnal, *Prog. Polym. Sci.* **2005**, *30*, 559.
- [21] A. J. Müller, Z. H. Hernández, M. L. Arnal, J. J. Sánchez, *Polym. Bull.* **1997**, *39*, 465.
- [22] A. J. Müller, R. M. Michell, R. A. Pérez, A. T. Lorenzo, *Eur. Polym. J.* **2015**, *65*, 132.
- [23] F. Chen, *Polymer* **2001**, *42*, 4579.
- [24] M. L. Arnal, V. Balsamo, G. Ronca, A. Sánchez, A. J. Müller, E. Cañizales, C. U. de Navarro, *J. Therm. Anal. Calorim.* **2000**, *59*, 451.
- [25] V. Virkkunen, P. Laari, P. Pitkänen, F. Sundholm, *Polymer* **2004**, *45*, 4623.
- [26] M. Kontopoulou, W. Wang, T. G. Gopakumar, C. Cheung, *Polymer* **2003**, *44*, 7495.
- [27] E. Carmeli, D. Tranchida, A. Albrecht, A. J. Müller, D. Cavallo, *Polymer* **2020**, *203*, 122791. <https://doi.org/10.1016/j.polymer.2020.122791>
- [28] T. F. J. Pijpers, V. B. F. Mathot, B. Goderis, R. L. Scherrenberg, E. W. van der Vegte, *Macromolecules* **2002**, *35*, 3601.
- [29] J. Varga, J. Menczel, A. Solti, *J. Therm. Anal.* **1976**, *10*, 433.
- [30] J. Varga, J. Menczel, A. Solti, *J. Therm. Anal.* **1979**, *17*, 333.
- [31] A. T. Lorenzo, M. L. Arnal, A. J. Müller, A. Boschetti de Fierro, V. Abetz, *Macromol. Chem. Phys.* **2006**, *207*, 39.
- [32] R. M. Michell, A. Mugica, M. Zubitur, A. J. Müller, Self-Nucleation of Crystalline Phases Within Homopolymers, Polymer Blends, Copolymers, and Nanocomposites. in *Polymer Crystallization I*, Vol. 276 (Eds: F. Auriemma, G. C. Alfonso, C. de Rosa), Advances in Polymer Science; Springer International Publishing, Cham **2015**, p. 215.
- [33] L. Sangroniz, D. Cavallo, A. J. Müller, *Macromolecules* **2020**, *53*, 4581.
- [34] E. Carmeli, S. E. Fenni, M. R. Caputo, A. J. Müller, D. Tranchida, D. Cavallo, *Macromolecules* **2021**, *54*, 9100.
- [35] M. Trujillo, M. L. Arnal, A. J. Müller, E. Laredo, S. Bredeau, D. Bonduel, P. Dubois, *Macromolecules* **2007**, *40*, 6268.
- [36] V. Balsamo, Y. Paolini, G. Ronca, A. J. Müller, *Macromol. Chem. Phys.* **2000**, *201*, 2711.
- [37] M. F. J. Pijpers, V. B. F. Mathot, *J. Therm. Anal. Calorim.* **2008**, *93*, 319.
- [38] Y. Feng, X. Jin, J. N. Hay, *Polym. J.* **1998**, *30*, 215.
- [39] M.-H. Kim, R. G. Alamo, J. S. Lin, *Polym. Eng. Sci.* **1999**, *39*, 2117.
- [40] H. Pasch, M. I. Malik, Crystallization-Based Fractionation Techniques. in *Advanced Separation Techniques for Polyolefins*, (Eds: H. Pasch, M. I. Malik), Springer Laboratory; Springer International Publishing, Cham **2014**, p. 11.
- [41] A. Ortin, B. Monrabal, J. Sancho-Tello, *Macromol. Symp.* **2007**, *257*, 13.
- [42] N. Aust, M. Gahleitner, K. Reichelt, B. Raninger, *Polym. Test.* **2006**, *25*, 896.
- [43] S. Anantawaraskul, J. B. P. Soares, P. M. Wood-Adams, *J. Polym. Sci., Part B: Polym. Phys.* **2003**, *41*, 1762.

SUPPORTING INFORMATION

Additional supporting information may be found in the online version of the article at the publisher's website.

How to cite this article: M. Góra, D. Tranchida, A. Albrecht, A. J. Müller, D. Cavallo, *J. Polym. Sci.* **2022**, *60*(24), 3366. <https://doi.org/10.1002/pol.20220104>